

Laser Percussion Drilling of High Temperature Alloy and Qualitative/Quantitative Characterization

Hongyu Zhang¹, Ming Zhou^{*1}, Yunlong Wang², Xiangchao Zhang³, Yu Yan⁴ and Rong Wang¹

¹State Key Laboratory of Tribology, Department of Mechanical Engineering, Tsinghua University, Beijing 100084, China.

²School of Material Science and Engineering, Jiangsu University, Zhenjiang 212013, China.

³Shanghai Engineering Research Centre of Ultra-Precision Optical Manufacturing, Fudan University, Shanghai 200438, China.

⁴Corrosion and Protection Center, Beijing University of Science and Technology, Beijing 100083, China.

E-mail: zhouming@tsinghua.edu.cn

In this study, a LASERTEC 80 PowerDrill manufacturing system was used to fabricate a series of holes on a high temperature alloy workpiece with percussion drilling strategy. The morphological and elemental evaluations of the holes were performed using a scanning electron microscope associated with an energy dispersive X-ray analysis, focusing on the formation of melting and spattering contents, recast layer, and micro-cracks. Additionally, a quantitative method based on Matlab programming was developed to characterize conicity and circularity of the holes, with the calculation of the apparent radius, the RMS deviation, and the maximum deviation. The results showed that more melting and spattering contents accumulated around the holes at the entrance end than the exit end. The formation of recast layer (thickness: 15 μm) and micro-cracks was detected along the side wall of the holes, with a significant increase in the contents of O, Nb, and Cr compared with the bulk material. The conicity and circularity of the holes were optimized at a laser power of 100-110 W and a beam expanding ratio of 4. In conclusion, the present study proposed an effective qualitative/quantitative characterization method, which could be used for the evaluation of hole quality in laser drilling.

DOI: 10.2961/jlmn.2017.03.0022

Keywords: laser drilling; percussion drilling; micro-crack; recast layer; high temperature alloy

1. Introduction

Laser manufacturing has been widely used to fabricate micro-features in various materials such as metal, ceramic, plastic, and semiconductor [1, 2]. Laser drilling, as a versatile and reliable technique, has been greatly advocated in the aerospace and automotive industries, where the mechanical parts with an amount of precision holes are required [3]. For example, it is employed to manufacture the shaped film holes, which form a protective cooling layer between the external surface of the engine components (e.g., turbine blade) and the hot gases [4]. Basically, three strategies are used in laser drilling, including percussion drilling, trepan drilling, and helical drilling.

In spite of the presence of thermal effect during drilling, short-pulsed lasers represent a good choice in many cases, with acceptable accuracy and efficiency [5, 6]. In the past few years, different methods have been developed in order to reduce the thermal effect. In the study performed by Kang et al., ultrasonic vibration was applied to a nanosecond laser machining process, and it was found to prevent the surface oxidation and the formation of recast layer [7]. Porter et al. proposed a water jet guided laser cutting technique, and investigated in detail the influence of various factors, e.g., cutting distance, incidence angle, and feed speed [8]. In addition, it was suggested by Hu et al. that a reduction in pulse duration down to picosecond scale

may overcome the thermal issues [9], and various holes with quite a good quality were manufactured by the present authors through a combination of picosecond laser and helical drilling [10].

From a review of previous research, although there are many studies investigating the laser-material interactions during laser drilling process, employing either simulation or experiment methods [11-13], it is considered that an intensive qualitative/quantitative characterization of the holes fabricated by laser drilling has been lacking [14]. Consequently, the present study aims to develop an effective method for qualitative/quantitative characterization of the laser-drilled holes.

2. Materials and methods

2.1 Experimental setup

A LASERTEC 80 PowerDrill manufacturing system integrated with a Nd:YAG laser (wave length: 1064 nm; maximum power: 300 W) was utilised to drill through holes on a high temperature alloy workpiece (model: GH169; thickness: 3.0 mm). The workpiece was polished to a surface roughness of ~ 30 nm using polyurethane polishing pad and diamond paste, and then fixed onto a five-axis positioning platform, which enables stable movement of the workpiece in the horizontal plane (accuracy: 10 μm). The percussion drilling strategy was

applied to drill a series of holes vertically at 90° to the workpiece, with the laser beam focusing on the top surface through a focusing lens (focal distance: 150 mm). The assist oxygen was supplied along the nozzle of the drilling head during manufacturing at a pressure of 0.4 MPa. Two experimental conditions were investigated on the quality of the holes: (1) laser power: 80~130 W; beam expanding ratio: 4; (2) laser power: 100 W; beam expanding ratio: 1~6. The experiment was repeated at least three times to ensure statistical validity, with the separation of two holes at 5 mm in order to avoid the thermal effects. The primary drilling parameters were summarized in Table 1.

Table 1 Laser percussion drilling parameter setup

Parameter	Value
Average power (W)	80-130
Repetition rate (Hz)	30
Pulse duration (ms)	1
Beam expanding ratio	1-6
Assist gas pressure (MPa)	0.4
Number of pulses	10

2.2 Morphological analyses of holes

Following laser percussion drilling experiment, the entrance end and the exit end of the holes were examined, without any treatment of the workpiece, using a Quanta 200 FEG scanning electron microscope (SEM, FEI, Netherlands) to directly detect the formation of melting and spattering contents surrounding the holes.

2.3 Quantitative analyses of holes

A program was developed using Matlab 7 to fit the edge of the holes at both the entrance end and the exit end from the SEM micrographs, based on the assumption that the hole boundary was composed of an amount of points with the greatest gradient [15]. Subsequently, the edge curve of the hole was fitted as a circle using the least squares method, so that the apparent radius of the hole could be determined. Furthermore, the conicity (nominated as the apparent radius of the entrance end divided by that of the exit end), the RMS deviation (nominated as the root-mean-squares value of the difference between the edge curve of the hole and the fitted circle), as well as the maximum deviation (nominated as the peak-to-valley value of the difference between the edge curve of the hole and the fitted circle) of the hole were calculated through the program, and the average values of these parameters were obtained for the holes manufactured under the same drilling conditions.

2.4 Morphological and elemental analyses of hole sections

The workpiece was further investigated using the SEM at an inclined angle of 20° in order to observe the formation of recast layer and micro-cracks along the side wall of the hole. Additionally, the workpiece was cut into small pieces by wire-electrode cutting, with each hole filled with EpoFix resin according to the manufacturer's instructions (Struers, Denmark). Eventually, the longitudinal section of

the hole was exposed following polishing treatment, and examined using the SEM associated with an energy dispersive X-ray (EDX) analysis for both morphological observation of the recast layer and elemental composition comparison between the bulk material and the recast layer.

3. Results and discussion

3.1 Formation of melting and spattering contents

The surface morphology of the entrance end and the exit end of the holes manufactured with different laser powers (80-130 W) and beam expanding ratios (1-6) was shown in Figures 1 and 2. It was obvious from the SEM micrographs that, in comparison with the original surface, the entrance end became much rougher due to the formation of a layer of melting and spattering contents accumulating around the holes. By contrast, the exit end was not greatly affected by the drilling process, with only the presence of detectable spattering debris on the surface. It was anticipated that the percussion drilling strategy was responsible for resulting in this phenomenon because the thick high temperature material could not be removed quite rapidly by the laser. At the entrance end all laser pulses generated material melting while at the exit end just the last laser pulses were pushing material, thus leading to the formation of less melting and spattering contents.

Additionally, it was indicated that the hole size generally demonstrated an increasing trend with the increase of laser power at both the entrance end and the exit end. However, the hole size fabricated under different beam expanding ratios basically presented a decreasing trend at the entrance end but an increasing trend at the exit end (except for the hole obtained at the beam expanding ratio of 1). From the morphological evaluation of the holes, it seemed that a laser power of 100-110 W and a beam expanding ratio of 3-4 represented a good parameter setup.

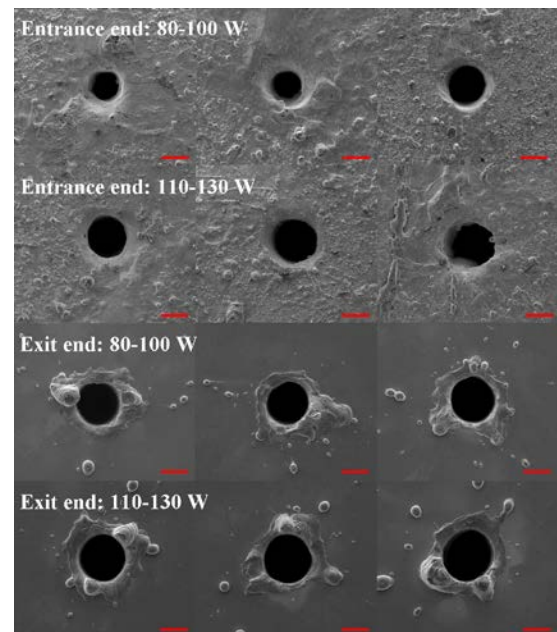


Fig. 1 SEM micrographs of the entrance end and the exit end of the holes drilled by different laser powers 80-130 W. Red bar: 0.2 mm.

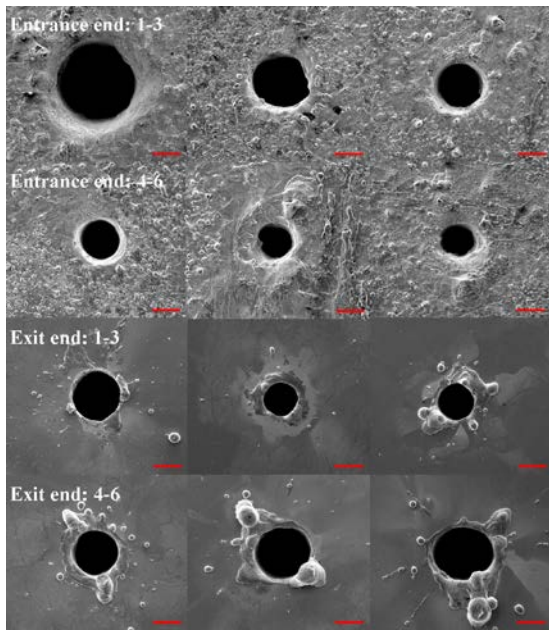


Fig. 2 SEM micrographs of the entrance end and the exit end of the holes drilled by different beam expanding ratios 1-6. Red bar: 0.2 mm.

3.2 Characterization of conicity, RMS deviation, and maximum deviation

A typical fitting of hole edge from the SEM micrograph through Matlab programming, which was represented by a white curve, was shown in Figure 3. This indicated that the boundary of the hole could be detected successfully employing this technique. The values of the apparent radius, the RMS deviation, and the maximum deviation of the holes fabricated with different laser powers (80-130 W) and beam expanding ratios (1-6) were shown in Figures 4

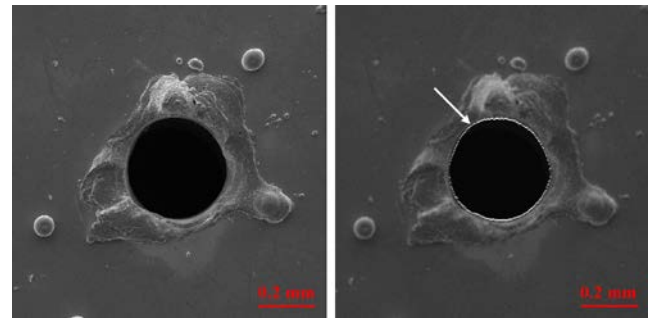


Fig. 3 Fitting of hole edge from SEM micrograph through Matlab programming based on gradient level extraction.

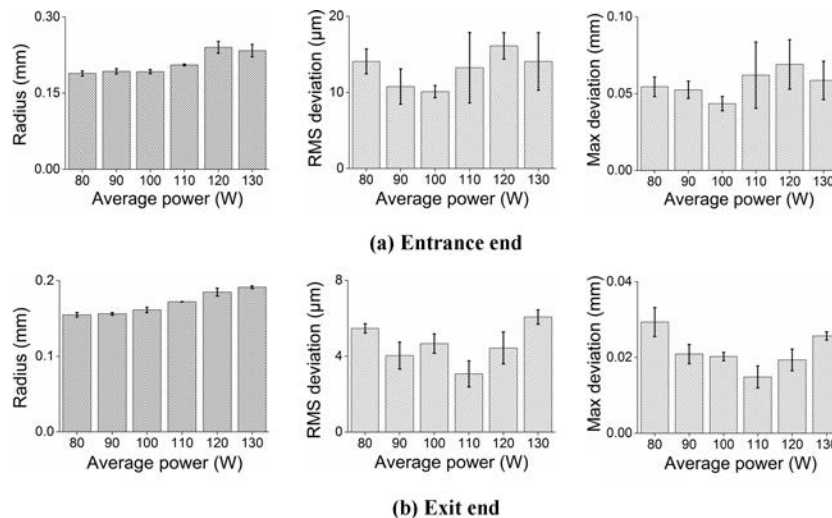


Fig. 4 The apparent radius, the RMS deviation, and the maximum deviation of the holes drilled by different laser powers 80-130 W.

3.3 Formation of recast layer and micro-cracks

The SEM micrographs shown in Figure 6 demonstrated clearly the formation of recast layer (a) and micro-cracks (b and c) along the side wall of the holes. This was attributed to the material removal process of short-pulsed laser, where a heat conduction mechanism primarily

dominated during laser drilling [16, 17]. An optimized parameter setup, such as laser power, focal position, assist gas pressure, etc., was reported to reduce the formation of recast layer and micro-cracks, and to improve the hole quality [18, 19]. Alternatively, the application of ultrafast lasers (e.g., picosecond or femtosecond lasers) was another

The variation of apparent radius was consistent with the visual observation from the SEM micrographs. The conicity of the holes was calculated as 1.22, 1.24, 1.19, 1.20, 1.30, and 1.22 for laser power of 80-130 W, and 2.38, 2.13, 1.61, 1.22, 0.96, and 1.70 for beam expanding ratio of 1-6. In addition, the RMS deviation and the maximum deviation of the holes reached the lowest values at the laser power of 100-110 W and the beam expanding ratio of 4. This suggested that an optimal conicity and circularity of the hole were obtained when the laser power was set at 100-110 W and the beam expanding ratio at 4. These results were also in compliance with the conclusions from morphological analyses of the holes.

The development of an effective method for quantitative characterization of the hole quality (in terms of conicity and circularity) based on Matlab programming was considered to be a valuable contribution of the present study. Through the fitting of hole edge by extraction of gradient level from the SEM micrograph, this method can be extensively used to characterize hole quality not only in laser drilling but also in other drilling conditions.

choice because material removal by these lasers was through direct evaporation, resulting in a significant reduction of the thermal effect and recast layer formation

[20-22]. However, the drilling efficiency would be compromised using the ultrafast lasers.

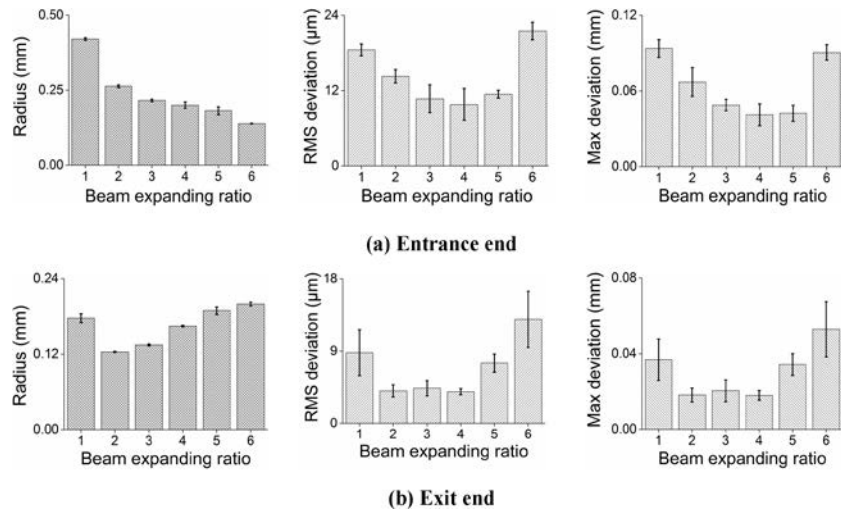


Fig. 5 The apparent radius, the RMS deviation, and the maximum deviation of the holes drilled by different beam expanding ratios 1-6.

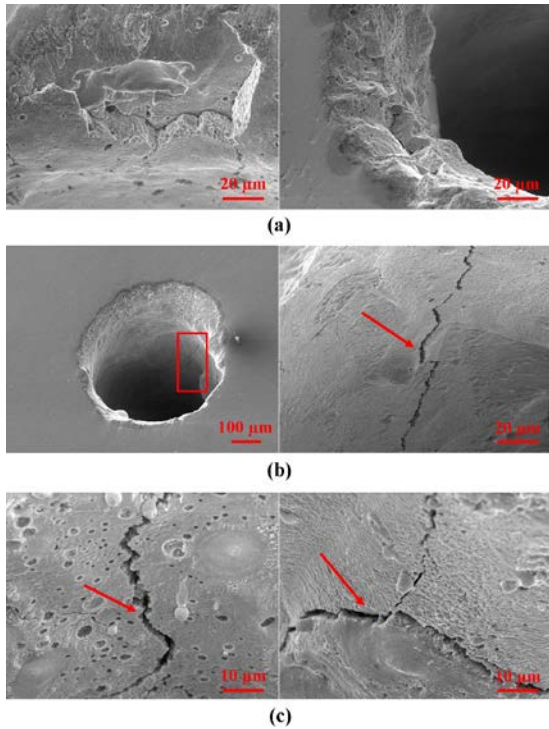


Fig. 6 Formation of recast layer and micro-cracks along the side wall of the holes: (a) laser power 90 W, beam expanding ratio 4; (b) laser power 100 W, beam expanding ratio 2; (c) laser power 120 W, beam expanding ratio 4.

A distinctive difference, in terms of morphological observation and elemental composition, between the bulk material and the recast layer was presented in the SEM micrograph of the longitudinal section of the holes, as shown in Figure 7. The thickness of the recast layer was approximately 15 µm. The comparison of elemental composition was displayed in Table 2 in detail. It was obvious that a great increase in the contents of O, Nb, and Cr was observed. It was considered that the melted material

was oxidized before it re-solidified along the side wall of the hole, resulting in the increase in the content of O [23]. In addition, the increase in the contents of Nb and Cr was related to the cooling process, because Nb and Cr tended to precipitate in a relatively slow cooling process (air cooling in the present study). As a result, the contents of Fe and Ni decreased significantly.

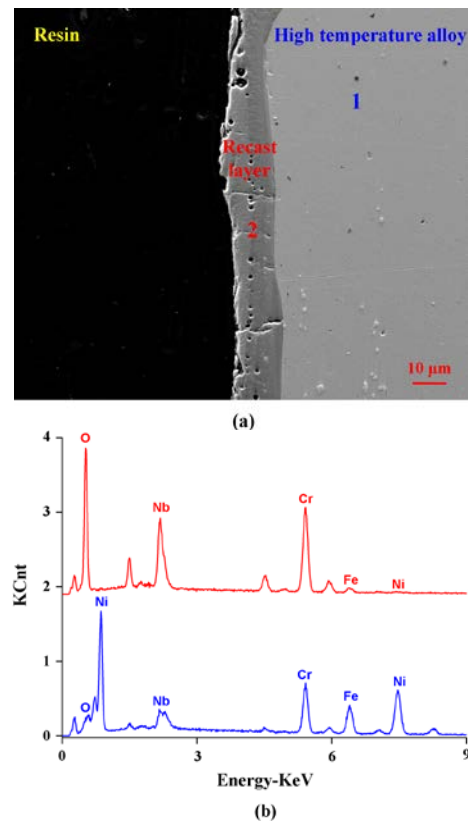


Fig. 7 Morphology and elemental composition comparison between bulk material (1) and recast layer (2), laser power 100 W, beam expanding ratio 1.

Table 2 Elemental composition (wt %) between the bulk material and the recast layer

Element	Fe	Ni	Cr	Nb	O	Others
Bulk material (1)	16.9	48.2	18.2	5.1	0.2	11.4
Recast layer (2)	3.4	1.5	36.9	18.0	24.5	15.7

4. Conclusions

The following conclusions can be drawn from the present study: (1) The accumulation of melting and spattering contents around the holes at the entrance end was observed, and the formation of recast layer and micro-cracks along the side wall was detected. This was attributed to heat conduction mechanism of short-pulsed laser during the material removal process; (2) The apparent radius, the RMS deviation, and the maximum deviation of the holes were calculated by Matlab programming. The holes with the optimal quality (conicity and circularity) were obtained at a laser power of 100-110 W and a beam expanding ratio of 4. (3) The method for quantitative characterization of hole quality developed in the present study could be widely used in laser drilling and other drilling conditions.

Acknowledgments

This study was supported by National Basic Research Program of China (Grant No. 2011CB013004), National Natural Science Foundation of China (Grant No. 51375008, 51675296), Tsinghua University Initiative Scientific Research Program (Grant No. 20151080366), and the Research Fund of State Key Laboratory of Tribology, Tsinghua University, China (Grant No. SKLT2015B03).

Appendix

```
function [Radius,RMS,PV]=HoleFit(filename,width,esize)
if nargin<3
    esize=1;
end
A=double(imread(filename));
A=A(:,end:-1:1);
if size(A,3)>1
    A=A(:,:,1)+A(:,:,2)+A(:,:,3);
end
sc=max(A(:));
A(A==sc)=median(A(:));
sc=min(A(:));
A(A==sc)=median(A(:));
NrR=size(A,1);
NrC=size(A,2);
spacing=width/(NrC-1);
C=A(2:NrR-1,:);
D=(A(3:NrR,:)+A(1:NrR-2,:))/2;
sc=diff(A);
sc=median(abs(sc(:)));
Noi=abs(C-D)>sc*2;
C(Noi)=D(Noi);
A(2:NrR-1,:)=C;
C=A(:,2:NrC-1);
D=(A(:,3:NrC)+A(:,1:NrC-2))/2;
Noi=abs(C-D)>sc*2;
C(Noi)=D(Noi);
A(:,2:NrC-1)=C;
B=A<(median(A(:))+2*min(A(:)))/3;
H=bwmorph(imdilate(B,strel('disk',10)), 'thin', Inf);
```

```
H=bwareaopen(H,10);
NrP=sum(H(:));
location=zeros(NrP,2);
[location(:,1),location(:,2)]=find(H);
H=imdilate(H,strel('disk',esize));
c=mean(location,1);
r=((location(:,1)-c(1)).^2+(location(:,2)-c(2)).^2).^0.5;
Radius=mean(r)*spacing;
RMS=std(r-Radius)*spacing;
PV=(max(r)-min(r))*spacing;
M=max(A(:))*2-min(A(:));
for k=1:NrP
    A(H)=M;
end
A=A(:,end:-1:1);
A=A(end:-1:1,:);
surf(A)
colormap gray
shading interp
view([0 0 1])
axis equal
axis tight
axis off
```

References

- [1] A. Barchanski, D. Funk, O. Wittich, C. Tegenkamp, B.N. Chichkov and C.L. Sajtí: J. Phys. Chem. C, 119, (2015) 9524.
- [2] J. Cheng, C.S. Liu, S. Shang, D. Liu, W. Perrie, G. Dearden and K.G. Watkins: Opt. Laser. Technol., 46, (2013) 88.
- [3] A. Ancona, D. Nodop, J. Limpert, S. Nolte and A. Tunnermann: Appl. Phys. A, 94, (2009) 19.
- [4] R.S. Bunker: J. Heat. Trans.-T ASME, 127, (2005) 441.
- [5] K.H. Leitz, B. Redlingshofer, Y. Reg, A. Otto and M. Schmidt: Physics. Procedia., 12, (2011) 230.
- [6] K.H. Leitz, H. Koch, A. Otto and M. Schmidt: Appl. Phys. A, 106, (2012) 885.
- [7] B. Kang, G.W. Kim, M. Yang, S.H. Cho and J.K. Park: Opt. Laser. Eng., 50, (2012) 1817.
- [8] J.A. Porter, Y.A. Louhisalmi, J.A. Karjalainen and S. Furger: Int. J. Adv. Manuf. Technol., 33, (2007) 961.
- [9] W.Q. Hu, Y.C. Shin and G.B. King: J. Manuf. Sci. E.-T ASME, 132 (2010) 1.
- [10] H.Y. Zhang, J.K. Di, M. Zhou, Y. Yan and R. Wang: Appl. Phys. A, 119, (2015) 745.
- [11] X.D. Wang, A. Michalowski, D. Walter, S. Sommer, M. Kraus, J.S. Liu and F. Dausinger: Opt. Laser. Technol., 41, (2009) 148.
- [12] J. Finger and M. Reininghaus: Opt. Express., 22, (2014) 18790.
- [13] U. Zywiets, C. Reinhardt, A.B. Evlyukhin, T. Birr and B.N. Chichkov: Appl. Phys. A, 114, (2014) 45.
- [14] I. Arrizubieta, A. Lamikiz, S. Martinez, E. Ukar, I. Taberero and F. Girot: Int. J. Mach. Tool. Manu., 75, (2013) 55.
- [15] V. Gonzalez-Castro, J. Debayle and J.C. Pinoli: Pattern. Recogn. Lett., 47, (2014) 50.
- [16] W. Schulz, U. Eppelt and R. Poprawe: J. Laser. Appl., 25, (2013) 012006.
- [17] D.S. Ivanov, A.I. Kuznetsov, V.P. Lipp, B. Rethfeld, B.N. Chichkov, M.E. Garcia and W. Schulz: Appl. Phys. A, 111, (2013) 675.

- [18] W.T. Chien and S.C. Hou: *Int. J. Adv. Manuf. Technol.*, 33, (2007) 308.
- [19] S. Leigh, K. Sezer, L. Li, C. Grafton-Reed and M. Cuttill: *Proc. IMechE-Part B: J. Engineering Manufacture.*, 224, (2010) 1005.
- [20] J. Kaspar, A. Luft, S. Nolte, M. Will and E. Beyer: *J. Laser. Appl.*, 18, (2006) 85.
- [21] M.S. Bello-Silva, M. Wehner, C. Eduardo, F. Lampert, R. Poprawe, M. Hermans and M. Esteves-Oliveira: *Laser. Med. Sci.*, 28, (2013) 171.
- [22] L. Jiang and H.L. Tsai: *J. Heat. Trans.-T ASME*, 127, (2005) 1167.
- [23] H.Y. Zhang, J.K. Di, M. Zhou and Y Yan: *Chin. J. Mech. Eng.-EN*, 27, (2014) 972.

(Received: September 15, 2016, Accepted: October 7, 2017)